Service Outage Estimation for Unmanned Aerial Vehicles

A Measurement-Based Approach

Lechuga, Melisa Maria Lopez; Sørensen, Troels Bundgaard; Wigard, Jeroen; Kovacs, Istvan; E. Mogensen, Preben

Published in:
IEEE Wireless Communications and Networking Conference 2022

DOI (link to publication from Publisher):
10.1109/WCNC51071.2022.9771599

Publication date:
2022

Document Version
Accepted author manuscript, peer reviewed version

Service Outage Estimation for Unmanned Aerial Vehicles: A Measurement-Based Approach

Melisa López*, Troels B. Sørensen*, Jeroen Wigard†, István Z. Kovács†, Preben Mogensen*†
*Aalborg University
†Nokia
mll@es.aau.dk

***Abstract*—One of the key enablers for the use of cellular networks to provide connectivity to Unmanned Aerial Vehicles (UAVs) is reliability assurance. Estimating accurately the expected service availability and reliability that a UAV will experience along a planned route, helps to avoid critical situations. In this paper, we evaluate the use of a data-driven approach to estimate the expected serving signal level of a UAV planning to fly along a specific path. The estimation approach, presented in a previous study for the ground-level case, is based on the aggregation of measurements of UAVs that have previously been flying along the same route. Using this approach we achieve an estimation error as low as 2.7 dB. Based on the estimations we calculate the expected outage probability in terms of service availability and reliability and provide estimations of the expected critical areas along the route. Results show that 90% of the availability and 65% of the reliability critical areas in the route can be accurately estimated.**

***Index Terms*—Data-driven RSRP estimation, UAV reliability, Outage probability.**

I. Introduction

The market potential for commercial applications which make use of Unmanned Areal Vehicles (UAVs), or drones, is rapidly increasing [1]. Most of these applications require the operation of drones Beyond Visual Line of Sight (BVLOS). Ubiquitous cellular networks are considered to be one of the main candidates to provide this service. Strict regulatory requirements enforced in standardization [2] have led to extensive research efforts to ensure that the network can provide reliable communication between the drone and its controller.

The existing literature focuses on pointing out the challenges of UAV communications over cellular networks and proposing techniques to overcome them [3]. Studies such as [4] and [5] point out the key role of interference in the performance of UAV communications. Potential solutions such as beamforming, are shown to be a good candidate to improve service reliability in [6]. In [7] and [8], the authors present the benefits of using a dual-operator hybrid access scheme to avoid outages caused by latency. Although there are solutions to improve UAV communications, the use of them is mostly based on reactive schemes. It would be beneficial for the service if the network could foresee the critical situation and proactively act against it. The Aerial Connectivity Joint Activity (ACJA) initiative proposes in [9] a two-phase operational context for UAVs. In the planning phase, RF conditions for the planned path are estimated, and in the flight phase, real-time radio Key Performance Indicators (KPIs) are monitored and used to estimate upcoming critical situations. Having beforehand information of a potential drop in the serving signal level or the Signal to Interference Ratio (SIR) could contribute to more efficient management of the network resources as well as more reliable User Equipment (UE) mobility and experienced Quality of Service (QoS) [10]. The most basic approach to obtain this information is to estimate, as accurately as possible, the Reference Signal Received Power (RSRP) that a UE will experience along a route that it is planning to fly through. There are well-known methods to estimate the radio coverage based on empirical and deterministic models such as ray-tracing. However, the estimation accuracy provided by these methods is poor [11].

In this paper, we present an outage estimation method that provides the network with in-advance information on the expected service availability and reliability along a route that a UAV is planning to fly. First, we evaluate the performance of a data-driven approach for serving signal level estimation, which was previously presented in [12] for ground-level scenarios. The estimation is evaluated using real LTE measurements and consists of the aggregation of RSRP samples recorded by UEs that have previously passed through the same location, regardless of the cell that they are connected to (i.e. *pre-service* estimation). We show how the estimations can be further corrected using RSRP recorded by the UE during the flight phase (i.e. *on-service* estimation). Furthermore, we use the serving RSRP estimations to obtain the expected service availability and reliability. With this information, the network can proactively act against upcoming areas where the signal level or the SIR are likely to drop (*critical areas*).

The paper is organized as follows: in Section II we include the description of the UAV radio measurements. In Section III we briefly describe the estimation approach. Results and conclusions are included in Sections IV and V, respectively.

II. UAV Radio Measurements

To evaluate the performance of the data-driven estimation approach we performed field UAV measurements at 50 m height in a rural scenario nearby the city of Aalborg in Denmark. The measurement route, as depicted in Fig.1, covered the last 5 km of a 15 km path (from X to Y) that was previously measured at ground-level [12]. In total, we performed eight round-trips in the 5 km route. The radio environment is characterized by scattered buildings with average heights

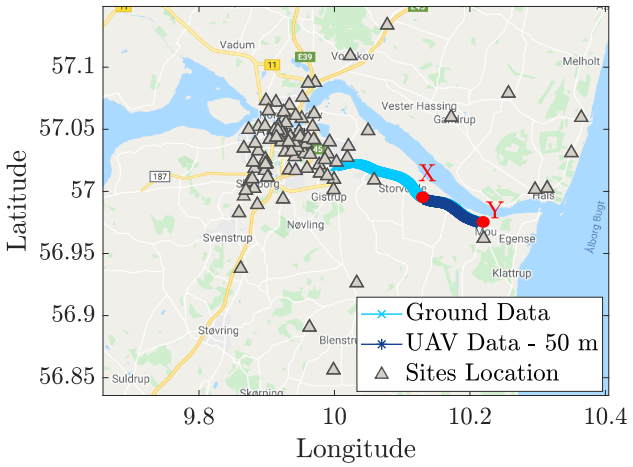

Fig. 1: Measurement routes and LTE base station sites in Aalborg, Denmark. X and Y mark the beginning and end of the UAV route, respectively.

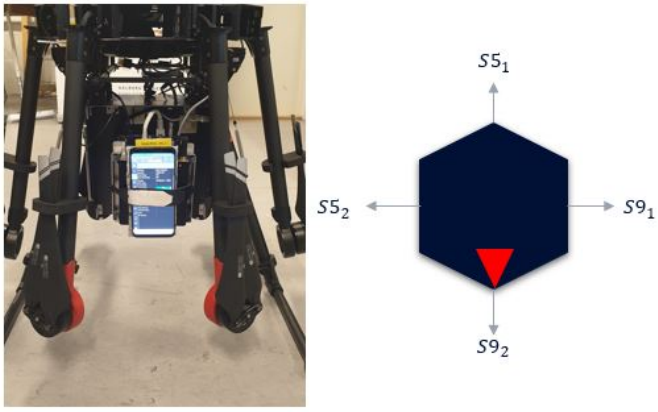

Fig. 2: Measurement setup (left) - DJI Matrice 600 drone front picture with one of the QualiPoc smartphones visible and (right) orientation scheme of UE positions where the red arrow indicates the drone flight direction.

below 10 m and a terrain profile with variation below 7 m. The measurements, which were conducted in a sparsely coveraged LTE network, are in the 1800 MHz band. The average inter-site distance of 8.3 km, base station heights range from 20 m to 39 m and down-tilts between 3 and 6 degrees.

The measurements were recorded using four commercial smartphones (2 Samsung Galaxy S5 and 2 Samsung Galaxy S9) with the QualiPoc© test firmware [13]. All of them were mounted underneath a drone, with each of the UEs oriented towards one of the four main compass directions, as shown in Fig. 2. The UEs recorded mainly the RSRP of the serving cell, and, in the case of the S5 model, also of the neighbors. An average number of 4 samples were recorded every 10 m.

III. Signal Level and Outage Estimation

The estimation approach used in this paper was previously presented in [12] for ground-level measurements. The serving RSRP values recorded by different UEs in a certain location are averaged (in dB scale) such that an estimation of the mean serving signal level that a UE is going to experience in that same location can be obtained. The estimation is location-based and should be valid for any UE regardless of the cell that it is connected to.

To evaluate this approach, the traces recorded by the UEs were organized along a 10-meter distance grid in $j = 1, ..., J$ segments. With a 5 km flight route, this led to a total of J = 500 segments. The mean value of all the measurements recorded by a UE in a certain grid segment j (4 samples on average, as mentioned in Section II) is used as the RSRP value recorded by that UE in segment j ($RSRP_{i,seg_j}$ in dB).

For every segment, the mean (in dBm) of all the serving RSRP values recorded by all the different UEs is used as the estimated value in that segment, i.e. the estimation in segment j is defined as:

$$\widehat{RSRP}_{seg_j} = \frac{1}{N}\sum_{i=1}^{N} RSRP_{i,seg_j} \quad \text{[dBm]} \quad (1)$$

The traces recorded by the UEs in opposite flying directions (X to Y and vice-versa) were considered as traces recorded by different UEs. With 4 measuring UEs and a total of 8 round-trips, the number of samples used to obtain the estimation in Eq. (1) equals N=32.

The precision of the signal level estimation is obtained by calculating, in each segment, the difference (in dB scale) between the estimation in that segment and each of the $N = 32$ actual recorded values. The distribution of this difference can be well approximated by a Gaussian distribution $\mathcal{N}(0, \sigma)$, where σ is the standard deviation of the estimation error (referred to as Δ).

A. Individual Offset Correction

To improve the performance of the estimation, we propose a method to correct the individual offset that a certain UE is observing with respect to the pre-service estimation in Eq. (1). To do this, we use real-time samples that the UAV is experiencing during the service (on-service estimation), as well as error distributions based on individual UEs that have previously passed through that same route. As for the aggregate distribution discussed above, the individual error distributions also have good approximation to a Gaussian with same standard deviation but different Mean Individual Offsets (MIOs) relative to the aggregate distribution mean. We use the z-test [14] as a parametric hypothesis test to determine whether a set of samples is likely to come from one of the individual error distributions.

Compared to the ground-level study case, where the MIO was stable along the route [12] and only a few samples at the beginning of the route allowed for *full-route* MIO correction, we observed that in the UAV case there is a need for updating the correction as the UAV moves along the route. This difference is most likely due to the higher impact of the directional antenna patterns of the UEs in the air compared to the ground. At a 50 m height and with good Line Of Sight (LOS) conditions, the number of cells that the UEs can observe

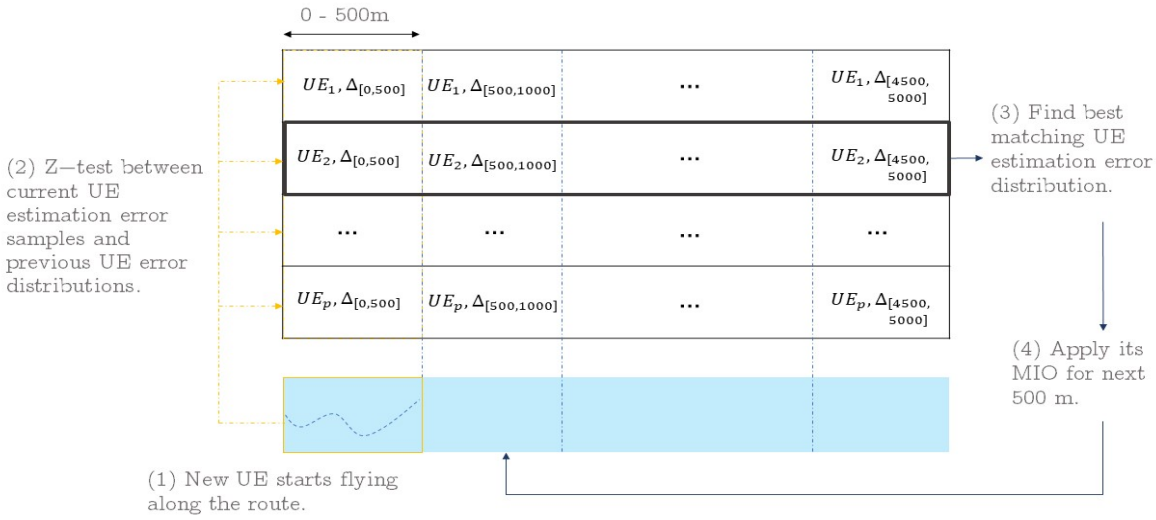

Fig. 3: Mean individual offset correction procedure.

is higher than at 1.5 m. Therefore, UEs in the same location but with different orientations in the air have higher probability to be connected to different cells and observe different signal levels.

To compensate for the variation of the MIO along the route, we update the offset estimation every d_{upd} = 500 m (*sliding window* MIO correction). We show in Fig. 3 the procedure for MIO correction, where the steps 1-4 indicate the order of the steps. When a UAV starts flying along the route (step 1), the samples observed within the first d_{upd} meters are tested against the stored distributions of each of the p UEs that have previously passed through that area (step 2).

The UE distribution with the highest p-value is selected (step 3) based on the z-test, and its MIO is used as a correction factor for the estimation in Eq. (1) (step 4). The hypothesis is tested every d_{upd} meters and the offset is corrected based on the latest observed samples.

B. Service Outage Probability

Since an accurate estimation error is observed after correcting the MIO of a UE, the serving RSRP estimations are further used to estimate the service availability and reliability that can be experienced along the route.

For *service availability*, we calculate the outage probability $P_{out,SA}$ that RSRP will drop below the availability threshold γ_{RSRP}. The probability is calculated as:

$$P_{out,SA} = P(RSRP < \gamma_{RSRP} | RSRP = \widehat{RSRP}) = \Phi(\frac{\gamma_{RSRP} - \widehat{RSRP}}{\sigma}) \quad (2)$$

Φ is the cumulative distribution function of the standard normal distribution and σ is the known standard deviation of that distribution. This equation follows from the observation that the estimation error distribution can be well approximated with a Gaussian.

For the *service reliability* estimations, we first estimate the SIR:

$$\widehat{SIR} = \frac{\hat{S}}{\hat{I}} = \frac{\widehat{RSRP_{SC}}}{\sum_{k=1}^{NC} \widehat{RSRP_k} \cdot \delta} \quad \text{[dB]} \quad (3)$$

$\widehat{RSRP_{SC}}$ is the serving cell signal level estimation, $\widehat{RSRP_k}$ the estimation of the $k = 1, ..., NC$ neighboring cells (NC = 5 strongest neighbors if available) and δ a fixed constant accounting for the impact of the traffic load.

The outage probability $P_{out,SR}$ that the SIR drops below a certain threshold γ_{SIR} is calculated following the same procedure from Eq. (2). Given the Gaussian shape of the estimation error, the linear value of the estimator $\widehat{RSRP}$ can be seen as a log-normal random variable with mean $\widehat{RSRP}$ and standard deviation σ. This is valid for both serving and interfering signals. The interference sum in the denominator of Eq. (3) will be approximately log-normal, as will the SIR ratio. Their statistics in the form of logarithmic mean and standard deviation can be calculated numerically by an extended version of the Schwarz & Yeh algorithm with account for correlated signals [15]. We calculate $P(SIR < \gamma_{SIR})$ assuming a correlation coefficient of 0.3 between the serving and interfering signals.

IV. Results

We first show the results obtained for the serving RSRP estimations using the data-driven approach. We aggregate the samples of $N = 32$ UE traces recorded to obtain an estimation that, as shown in Fig. 4a, presents an overall estimation error of 4.9 dB for the pre-service stage. We compare these results with the ones observed in the ground-level case in Table I. For reference, we also include the shadow fading values at area level. Since the estimations obtained with the data-driven approach are location-based, the estimation accuracy is below the shadow fading in the area. Due to the improved visibility

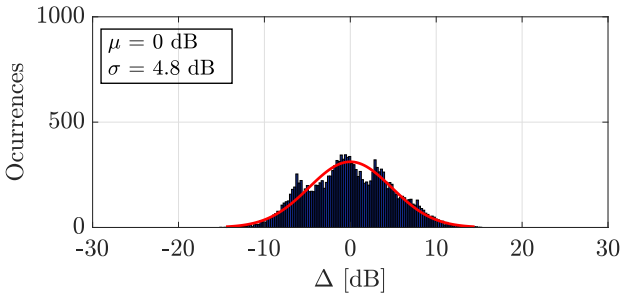

(a) Before MIO

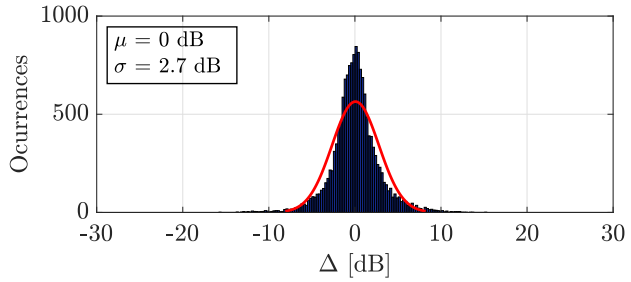

(b) After MIO

Fig. 4: Data-driven approach estimation error Δ [dB] before (a) and after (b) MIO correction.

conditions of the drone, and the lack of obstacles between the transmitter and the receiver, shadow fading for the UAV (4.3 dB) is almost 3 dB lower than at ground-level (7.2 dB).

Results in [12] show an overall estimation error of 6.3 dB at ground-level. The fit in the UAV case is not so obvious as the error distribution seems to present multiple modes, which are most likely caused by the different signal levels experienced by UEs oriented towards different directions. This leads to differences when correcting the MIO in the air. At ground-level, the stability of the offset for a specific UE oriented towards a certain direction allowed for the correction to be performed at the beginning of the route and be valid for the rest of it (*full-route* MIO correction). This method is not valid in the UAV case as the MIO of the whole route varies along the route and the samples observed for the z-test are not able to find a matching error distribution to the ones stored in the database (from UEs that have previously passed through the same route). Therefore, as explained in Section III-A, MIO correction needs to be updated along the route. For the results presented here, $p = N * 0.75$, i.e. 25% (eight) of the available traces were used for testing the correction approach, with eight random traces in every testing round until all of them were tested. Results in Fig. 4b show that not only the standard deviation of the estimation error is reduced to 2.7 dB, but also the distribution is uni-modal and symmetric now that the offsets due to directivity have been removed. Although the distribution is clearly more peaked than a Gaussian, we keep that assumption for simplicity in the sequel. We also include in Table I the results for *sliding window* MIO correction at ground-level. The difference when using the *full-route* correction is 0.3 dB (5.1 dB vs 4.8 dB).

TABLE I: Results Summary: Ground Level vs. UAV

	Ground Level	**UAV**
Data-Driven Δ [dB] *Before MIO Correction*	6.3	4.8
Data-Driven Δ [dB] *Full-route MIO Correction*	5.1	-
Data-Driven Δ [dB] *Sliding Window MIO Correction*	4.8	2.7
Shadow Fading [dB] *(Areal Level)*	7.2	4.3

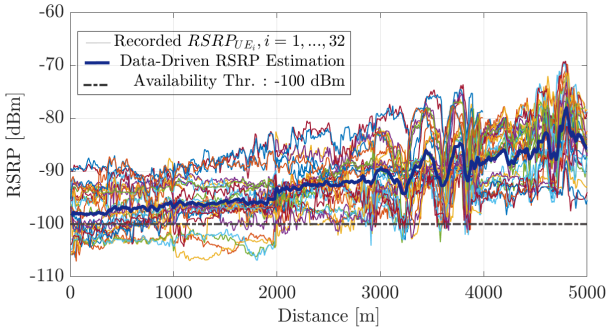

Fig. 5: N = 32 recorded traces and data-driven serving RSRP estimation.

This indicates that the sliding window approach has a low impact as the error is stable along the whole route.

A. Service Outage Estimation

Achieving a high accuracy of 2.7 dB allows us to further use the serving RSRP estimations to estimate the expected service availability and reliability as per (2) and (3). Fig. 6 shows the results for service availability when using γ_{RSRP} = -100 dBm. For reference, we include in Fig. 5 the 32 serving RSRP traces recorded in the 5 km route along with the estimation and the threshold. In Fig. 6a, we choose three example UEs pointing towards different directions (and with different MIOs) to show the effects of MIO correction. As it can be seen, the corrected estimation traces in the on-service stage follow the trend of the actual ones better than the pre-service estimation. This is also observed in Fig. 6b, where the outage probability for service availability is shown. If we choose UE A as a reference, we observe that the actual recorded RSRP level is below -100 dBm up to approximately two kilometers, in agreement with the estimated outage probability. For UE C, on the other hand, the actual trace is shown to be above the threshold along the whole route. Contrary to what was initially estimated in the pre-service stage, where almost half of the route would be declared critical, the on-service stage estimates a very low service availability outage probability for UE C.

To evaluate the performance of the outage probability estimations, we classify the segments into critical (true positive or critical area) and non-critical (true negative or non-critical area). We use True Positive Rate (TPR), True Negative Rate (TNR), False Negative Rate (FNR), and False Positive Rate (FPR) for evaluation, as these metrics are typically used for classification methods [16]. Other metrics such as accuracy and F1-score have not been included as they were considered to be misleading for the purpose of our evaluation due to

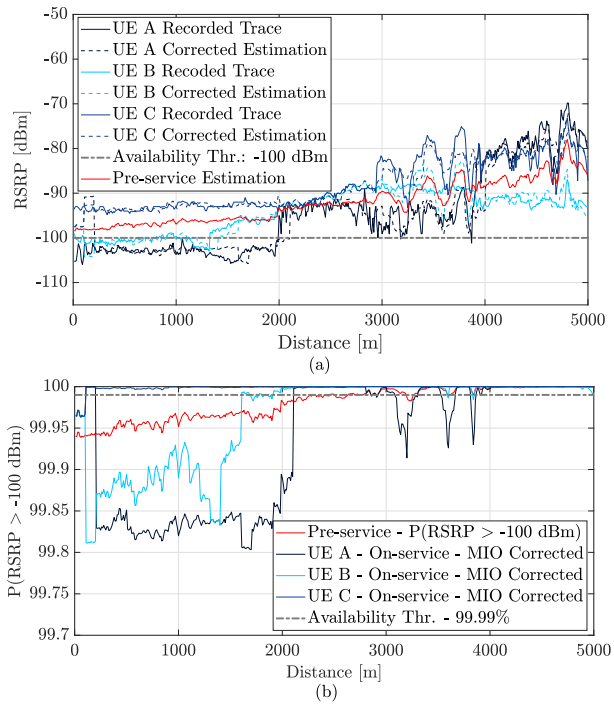

Fig. 6: Service Availability: (a) real and estimated traces of three example UEs and (b) outage probability estimations based on pre-service and on-service estimations for the three example UEs.

the low number of critical areas (unbalanced dataset). Our main objective is to obtain the highest TPR possible, which indicates the number of positives that are correctly classified, i.e. the number of critical areas that are correctly estimated since both service availability and reliability outages would be very critical for UAV communication. However, we would also like to reduce as much as possible the FPR, i.e. the number of incorrectly classified critical areas (false alarms), since that may lead to inefficient resource management (e.g. unnecessary resource reservation). Results are shown in Table II. Service availability estimations show an 81% TPR and a high FPR of 50% in the pre-service stage. However, in the on-service stage, almost 90% of the service availability critical areas can be estimated while observing only 20% of false alarms. As observed in Fig. 5, the number of samples dropping below the threshold is small (approximately 10%) compared to the total number of samples

For the service reliability estimations we first calculate, following Eq. (3), the SIR for each of the 16 UE traces at

TABLE II: Accuracy of service availability and reliability outage areas estimation.

	TPR [%] (Hit Rate)	**TNR** [%] (Specificity)	**FNR** [%] (Miss Rate)	**FPR** [%] (Fall-Out)
Availability *Pre-service*	81.1	49.9	18.9	50.1
Availability *On-service*	88.4	76.6	11.6	23.4
Reliability *Pre-service*	68.8	71.5	31.2	28.5
Reliability *On-service*	66.9	76.8	33.1	23.2

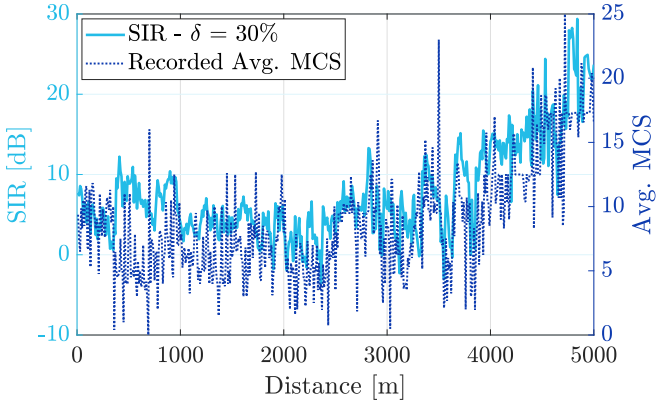

Fig. 7: Comparison of estimated SIR with δ = 30% with the recorded Avg. MCS trends(example UE).

which the strongest neighbors RSRP were also recorded ($S5$ smartphones). The SIR is calculated using an estimation of low, medium, and high load values (10%, 30%, and 60%, respectively). Fig. 8a shows the resulting SIR traces for δ = 30% and the corresponding threshold γ_{SIR} = -3 dB. The SIR is obtained by estimating the same load for all neighboring cells. To show that this is a fair representation of the actual quality experienced by the UAV, we include Fig. 7. We compare an example UE trace of the calculated SIR (with δ = 30%) and the corresponding recorded average Modulation and Coding Scheme (MCS), which the is selected by the UE proportionally to the data channel SIR. As it can be observed, the trends observed in the average MCS trace are also followed by the calculated SIR. On that basis, we calculate the service reliability outage probability using the approach explained in Section III-B. Results in Fig. 8b show that the outage probability increases with the load in the network. It can also be observed how the δ = 30% outage probability estimation matches best the SIR calculated traces in Fig. 8a. As previously done for service availability, the performance of the estimations is shown using the classification metrics. Table II shows that 69% of the critical areas are correctly estimated in the pre-service stage with an FPR of 28%. The TPR slightly decreases to 67% in the on-service stage, but so does the FPR to 23%. The benefits of MIO correction are not so obvious for the service reliability estimations as the MIO correction is only performed for the serving cell. MIO correction was not possible for the neighbors due to the very different error distributions observed from previous UEs (high number of cells observed).

V. Discussion and Conclusions

The estimation results shown in Section IV contribute to ensuring reliable communication between the UAV and its controller. Seen in the ACJA operational context to ensure reliable communication, the network can consider the pre-service estimations to decide whether the UAV can start the service or it should re-plan the route. Furthermore, the on-service estimations can contribute to more proactive and seamless UE mobility and QoS management. Decisions such as activating dual connectivity or an interference mitigation

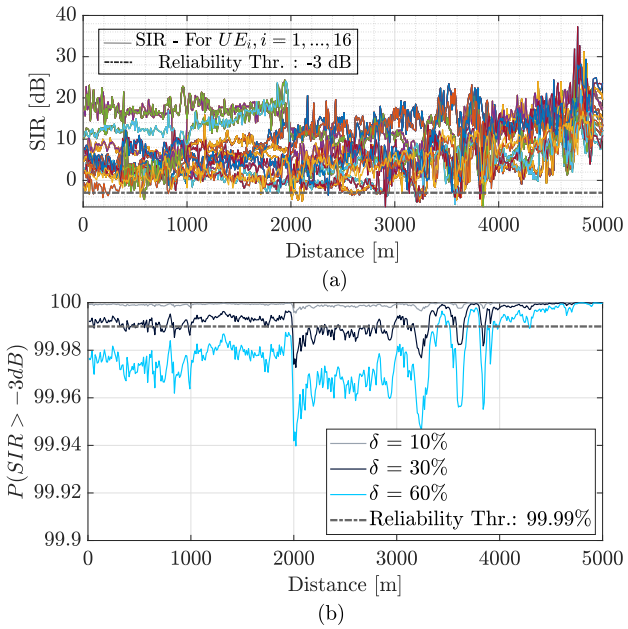

Fig. 8: Service Reliability: (a) N = 16 SIR traces estimated based on actual values and (b) outage probability estimation based on pre-service estimation.

technique can be made in advance, i.e., before the signal level or the quality of service is degraded.

In this paper, we discuss the use of a data-driven approach to estimate the expected serving signal level of a UAV along a planned path. The data-driven estimation consists of aggregating measurements from UEs that have previously passed through the same location. The method provides an overall accuracy of 4.9 dB.

The error can be further reduced to 2.7 dB by proactively correcting the MIO of the flying UAV with respect to the overall estimation. The correction is done using error distributions from previous UEs and updated based on observations of the most recent samples. The data-driven estimation approach and the MIO correction procedure require data from previous UEs to be available, limiting the use of these approaches.

With an accurate estimation of the serving RSRP, the network is able to calculate the expected service outage probability in terms of availability and reliability. The estimations show that almost 90% of the expected critical areas along the route in terms of availability can be detected in advance, showing only 20% of false alarms. For service reliability, the network would be able to detect almost 70% of the critical areas, maintaining the fall-out rate below 25%.

Acknowledgment

The authors would like to thank Telenor (Denmark) for supporting this work by sharing the network information. We would also like to express gratitude to Steffen Hansen, our drone pilot, and other colleagues at Aalborg University for the help provided during the measurement campaign.

References

[1] Godage, L. Global Unmanned Aerial Vehicle Market (UAV) Industry Analysis and Forecast (2018–2026); Montana Ledger: Boston, MA, USA, 2019.

[2] Study on Enhanced LTE Support for Aerial Vehicles (Release 15), 3GPP TR 36.777 V0.4.0 (2017-11), Technical Specification Group Radio Access Network, 2017.

[3] Fotouhi, A., Qiang, H., Ding, M., Hassan, M., Giordano, L. G., Garcia-Rodriguez, A., and Yuan, J., "Survey on UAV Cellular Communications: Practical Aspects, Standardization Advancements, Regulation, and Security Challenges," in IEEE Communications Surveys & Tutorials, vol. 21, no. 4, pp. 3417-3442, Fourthquarter 2019.

[4] H. C. Nguyen, R. Amorim, J. Wigard, I. Z. KováCs, T. B. Sørensen and P. E. Mogensen, "How to Ensure Reliable Connectivity for Aerial Vehicles Over Cellular Networks," in IEEE Access, vol. 6, pp. 12304-12317, 2018.

[5] H. Marques, P. Marques, J. Ribeiro, T. Alves and L. Pereira, "Experimental Evaluation of Cellular Networks for UAV Operation and Services," 2019 IEEE 24th International Workshop on Computer Aided Modeling and Design of Communication Links and Networks (CAMAD), 2019.

[6] T. Izydorczyk, M. Bucur, F. M. L. Tavares, G. Berardinelli and P. Mogensen, "Experimental Evaluation of Multi-Antenna Receivers for UAV Communication in Live LTE Networks," 2018 IEEE Globecom Workshops (GC Wkshps), 2018.

[7] R. Amorim, I. Z. Kovacs, J. Wigard, G. Pocovi, T. B. Sorensen and P. Mogensen, "Improving Drone's Command and Control Link Reliability through Dual-Network Connectivity," 2019 IEEE 89th Vehicular Technology Conference (VTC2019-Spring), 2019.

[8] Güldenring, J., Gorczak, P., Eckermann, F., Patchou, M., Tiemann, J., Kurtz, F., Wietfeld, C. (2020). Reliable long-range multi-link communication for unmanned search and rescue aircraft systems in beyond visual line of sight operation. Drones, no. 4(2).

[9] Interface for Data Exchange between MNOs and the UTM Ecosystem: Network Coverage Service Definition, v1.00. ACJA, GSMA and GUTMA approved version. February 2021.

[10] Bui, Nicola. "Prediction-based techniques for the optimization of mobile networks." (2017).

[11] J. Thrane, D. Zibar and H. L. Christiansen, "Comparison of Empirical and Ray-Tracing Models for Mobile Communication Systems at 2.6 GHz," 2019 IEEE 90th Vehicular Technology Conference (VTC2019-Fall), 2019.

[12] M. Lopéz, T. B. Sørensen, I. Z. Kovács, J. Wigard and P. Mogensen, "Experimental Evaluation of Data-driven Signal Level Estimation in Cellular Networks," 2021 IEEE 94th Vehicular Technology Conference (VTC2021-Fall), 2021.

[13] R&S Test Equipment Information. TSME radio network scanner and QualiPoc Android test devices manual, 2020.

[14] Kitchens, L.J. 2003. Basic Statistics and Data Analysis. Duxbury. ISBN 0-534-38465-X.

[15] Intelligent Distributed Antenna Systems (IDAS); Assessment by measurement and simulation", Ph.D. Dissertation, Troels B. Sørensen, Aalborg University, February 2002.

[16] Hossin, M., and Sulaiman, M. N. (2015). "A review on evaluation metrics for data classification evaluations." International journal of data mining knowledge management process 5.2 (2015): 1.